https://doi.org/10.2352/ISSN.2470-1173.2017.18.COLOR-041

Color halftoning based on Neugebauer Primary Area Coverage*

Wanling Jiang[1], *Weijuan Xi*[1], *Utpal Sarkar*[2], *Robert Ulichney*[3], *and Jan P. Allebach*[1]
[1] *Electronic Imaging Systems Laboratory, School of Electrical and Computer Engineering, Purdue University, West Lafayette, IN-47906, U.S.A.* {*jiang267,xi9,allebach*}*@purdue.edu;*
[2] *Hewlett-Packard Barcelona Division, Barcelona, Spain;*
[3] *Hewlett-Packard Laboratories USA, Cambridge, MA 02142, U.S.A.*

Abstract

Abstract—In this paper, we propose a halftoning method with Neugebauer Primary Area Coverage (NPAC) direct binary search (DBS), with the optimized human visual system (HVS) model, we are able obtain homogeneous and smooth hafltone colored image. The halftoning is based on separating the colored image represented in Neugebauer Primary in three channels based on human visual system, with swap-only DBS, we arrange the dots to bring the error metric to its minimum and the optimized halftone image is obtained. The separation of chrominance HVS filters between red-green and blue-yellow channels allows us to represent HVS more accurately. Color halftone images generated using this method and method of using combined chrominance filter is compared.

Introduction

[0]

Halftoning is used to represent different tone by placing black dots on a white surface. Due to the low pass nature of the human eye, the dots became invisible when viewed from a distance. Similarly, digital color halftoning converts continuous tone images to images comprising pixels with limited amount of colorants, ideally with minimal compromise of the image quality. Unlike traditional halftoning, digial color halftoning does not only represent the origianl image as traditional black and white halftoning does, but the color representation needs to be as close to the original image as possible.

There are several major color halftoning methods, the method that require the least computation is memoryless operation, processing each pixel at a time and do not revisit pixel, an example of this method is using selection matrix, in this method, each pixel is represented by Neugebauer Primary area coverage (NPAC), which will be introduced in section IV. Using the value given by the selection matrix, we can select the Neugebauer Primary (NP) for the pixel. A halftoned image represented by NPs is generated if we repeat this process for all the pixels. Since ach NP corresponds to a unique sRGB value, we can represent the halftoned image in sRGB colorspace. This method is similar to screening method, which is also based on pixel by pixel comparison. Both method require only the minimal computation among all the methods of halftoning.

Another halftoning method require the information of a neighborhood pixels and thus has more computation but have better hafltoning quality, an example of this type of halftoning is error diffusion. In this method, each pixel diffuse the error to its nearby pixels, or each pixel collect the error information from its neighboring pixels, the difference from previous methods is that it each pixel have information of its neighborhood, thus yield halftone images with better quality. This method only have single pass through the entire image, no iteration needed.

The most computationally expensive one is iterative method, the image is visited multiple times, an example of this method is DBS. There are two categories of DBS in terms of the graininess of the dots, dispersed-dot and clustered-dot DBS. Both methods render good halftone image, the difference between them is that clustered-dot DBS generates courser grained halftone images, which is suitable for printers that can not print stable pixels, while dispersed-dot DBS render finer gained halftone images, and is suitable for printers that can print stable pixels. The method used in this paper is dispersed-dot DBS. DBS algorithm takes into account the human visual system (HVS), which is low pass filter. DBS algorithm optimize halftone by bringing the gap between the filtered error between continuous and halftoned image down by performing swap and toggle of the pixels in the halftone image. If both swap and toggle are permitted, the tone of the initial halftone image is not preserved, however, if only swap is permitted, the tone of the initial halftone image is preserved. In this paper, swap-only DBS is adopted. In DBS, we have observed that the initial halftone have impact on the final halftone image quality. With DBS generated initial halftone, the final halftoned image has better quality than using random initial halftone.

Our work, NPAC-DBS halftoning, is based on the work of Je-Ho Lee[1] and A. Ufuk Agar[2], where color DBS is based on Neugebauer Primaries, and the algorithm operates in $Y_yC_xC_z$ color space. We first take an image in sRGB color space, then transfer to NPAC image set, which represent the continuous tone image in Neugebauer Primary color space, and finally use swap only NPAC DBS to obtain the halftoned image.

The rest of the paper is arranged as follows: In section II, we introduce the HVS models, compared them in spa-

[0]*Research sponsored by HP Inc., Barcelona, Spain

tial and frequency domain and also compared their color halftoning result. We also explored luminance channel amplification factor and perform color DBS in different color spaces. In section III, we describe how the initial halftone is generated, and similarly, how selection matrix method is applied. And then derive the error metric and the way to evaluate trial swap. In section IV, we talk about the pipline of getting NPAC image set from sRGB continuous image. In section V, we compared the experiment results. In section V, we draw the conclusion.

Human Visual System Model

We adopt the HVS model in $Y_yC_xC_z$ color space is based on CIE L*a*b* uniform color space which is used by Flohr et al.[3], this color space is defined using CIE XYZ as:

$$\begin{aligned} L^* &= 116 f(\frac{Y}{Y_n}) - 16 \\ a^* &= 200[f(\frac{X}{X_n}) - (\frac{Y}{Y_n})] \\ b^* &= 500[f(\frac{Y}{Y_n}) - f(\frac{Z}{Z_n})] \end{aligned} \tag{1}$$

Where X_n, Y_n, Z_n represent CIE XYZ tristumulus values , and $f(x)$ is defined by:

$$f(x) = \begin{cases} 7.787x + \frac{16}{116}, & 0 \le x \le 0.008856 \\ x^{1/3}, & 0.008856 < x \le 1. \end{cases} \tag{2}$$

In the above equation, L^* corresponds to luminance and a^* and b^* corresponds to chroma and hue respectively. The probram with CIE L*a*b* is it doesn not preserve the spatial averaged tone, so linearized CIE L*a*b* color space is used by Flohr et all.[3] and they denote it by $Y_yC_xC_z$:

$$\begin{aligned} Y_y &= 116\frac{Y}{Y_n} \\ C_x &= 200[\frac{X}{X_n} - \frac{Y}{Y_n}] \\ C_z &= 500[\frac{Y}{Y_n} - \frac{Z}{Z_n}] \end{aligned} \tag{3}$$

Where Y_y represent luminance, and C_x and C_z represent red-green and blue-yellow channel respectively.

Nasenan's HVS model

For luminance channel, we can use NasananâĂŹs model, the spatial frequency domain response is given by:

$$H_{Y_y}(u,v) = a\Gamma^b exp(-\frac{\sqrt{u^2+v^2}}{\lfloor c\ln\Gamma + d \rfloor}) \tag{4}$$

Were $a = 131.6$, $b = 0.3188$, $c = 0.525$, $d = 3.91$, and Γ is the average luminance of the light reflected from the print in cd/m^2, usually set to 11, and u and v are the spatial frequency coordinates in cycles/degree subtended at the retina.

Chromiance channel models based on data collected by Mullen

For the chrominance channels, the blue-yellow channel spatial frequency domain response is based on approximation by Kolpatzik and Bouman to experimental data collected by Mullen:

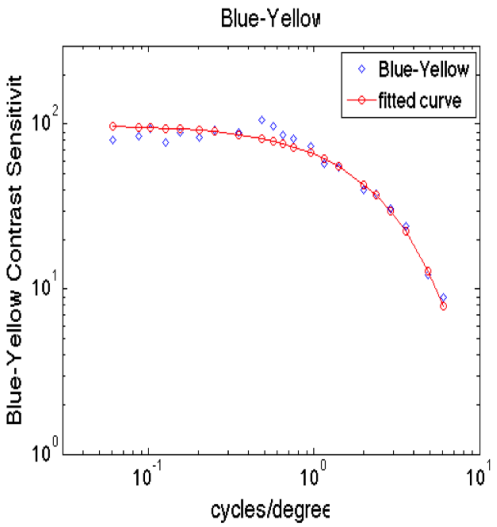

Figure 1. *The blue-yellow channel CSF*

The diamond mark in Fig. 1 represents the sampled data from Mullen's blue-yellow CSF figure, and the red curve is the fitted curve according to the samples. The contrast sensitivity is given as:

$$H_{C_z}(u,v) = Aexp(-\alpha\sqrt{u^2+v^2}) \tag{5}$$

Where $\alpha = 0.419$ and $A = 100$, and u and v are the spatial frequency coordinates in cycles/degree subtended at the retina.

Different from using blue-yellow channel filter for both red-green and blue-yellow channels, we use separate red-green channel filter based on the experimental data collected by Mullen[8]:

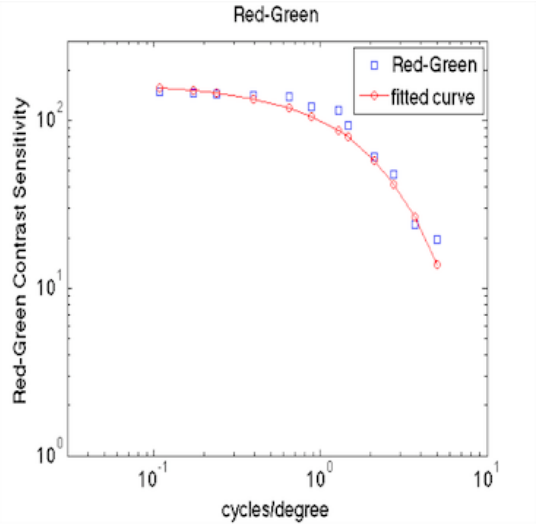

Figure 2. *The red-green channel CSF*

The square mark in Fig. 2 represents the sampled data from Mullen's red-green CSF figure, and the red curve is the fitted curve according to the samples. This spatial frequency domain model is approximated by:

$$H_{C_x}(u,v) = Aexp(-\alpha\sqrt{u^2+v^2}) \tag{6}$$

Where $\alpha = 0.497$ and $A = 165$, and u and v are the spatial frequency coordinates in cycles/degree subtended at the retina.

Wandell's HVS model

Except from Nasanen's luminance channel filter and Mullen's chrominance channel filters, we also examined Wandell's filters.[4] Wandell's $O_1O_2O_3$ color space in terms of CIE XYZ is[4]:

$$\begin{bmatrix} O_1 \\ O_2 \\ O_3 \end{bmatrix} = \begin{bmatrix} 0.279 & 0.72 & -0.107 \\ 0.449 & -0.290 & 0.077 \\ 0.086 & -0.590 & 0.501 \end{bmatrix} \begin{bmatrix} X \\ Y \\ Z \end{bmatrix} \tag{7}$$

Wandell's spatial kernel is given by:

$$f = k\sum_i \omega_i E_i \tag{8}$$

Where $E_i = k_i exp[-\frac{x^2+y^2}{\sigma_i^2}]$. The scale factor k_i is chosen so that E_i sums to 1. the scale factor k is chosen so that for each color plane, its two-dimensional kernel f sums to one. The parameters (ω_i, σ_i) for the three color planes are:

Where spread is in degrees of visual angle.[4]

Wandell's filter with respect to angular degree could not be applied to digital image, we need to generate descrete Wandell filter. Let x_d, y_d be the coordinates in

Wandell filter parameters

Plane	Weights ω_i	Spreads σ_i
Luminance	0.921	0.105
	0.105	0.133
	-0.108	4.336
Red-green	0.531	0.0392
	0.330	0.494
Blue-yellow	0.488	0.0536
	0.371	0.386

angular degrees subtended at the retina, the point spread function in terms of the angular degrees is:

$$p_r(x_d, y_d) = exp(-\frac{x_d^2+y_d^2}{\sigma^2}) \tag{9}$$

Assume that the viewing distance is D (inches), and x_p,y_p (in inches) are the coordinates on a paper at viewing distance D:

$$x_p = D \cdot x_d \cdot \frac{2\pi}{360} \tag{10}$$

The HVS with respect to x_p, y_p is:

$$p_p(x_p, y_p) = \exp\left(-\frac{x_p^2+y_p^2}{\left(\frac{2\pi\sigma D}{360}\right)^2}\right) \tag{11}$$

Let Δ be the sampling interval in plane of paper, and $R = \frac{1}{\Delta}$, then

$$p_d[m,n] = \exp\left(-\frac{m^2+n^2}{\left(\frac{2\pi\sigma S}{360}\right)^2}\right) \tag{12}$$

Where S is the scaling factor, and $S = R \cdot D$, $m, n = 0, 1, ..., 13$.

Daly's Luminance channel model

Sang Ho Kim and Allebach [5] compared Daly's contrast sensitivity function with Nasenan's model. Here we also examined Daly's luminance channel filter, its spatial frequency domain model is given by:

$$H(\bar{\rho}) = \begin{cases} a(b+c\bar{\rho})\exp(-(c\bar{\rho})^d), & \rho > \bar{\rho} \\ 1, & else. \end{cases} \tag{13}$$

Where spatial frequency $\bar{\rho}$ has unit of cycles/degree, $a = 2.2$, $b = 0.192$, $c = 0.114$, $d = 1.1$, $\bar{\rho}_{max} = 6.6$. In order to get 2-D frequency domain model, we replace $\bar{\rho}$ by $\sqrt{\bar{u}^2+\bar{v}^2}$, where $\bar{u}, \bar{v}$ are in cycles/degree. We cannot directly use Daly's spatial frequency domain filter, but after 2-D inverse fourier transform, we are able to apply it to our purpose as spatial domain luminance filter $h[x_d, y_d]$, where x_d, y_d are in angular degrees subtended at the retina. Follow similar derivation of (9-10), we get the HVS point spread

functions $\tilde{p}_i(x_p, y_p)$, $i = Y_y, C_x, C_z$, where x_p, y_p have units of in viewed at a distance D (inches).

$$\tilde{p}_i(x_p, y_p) = \frac{1}{D^2} h_i(\frac{180}{\pi D x_p}, \frac{180}{\pi D y_p}) \quad (14)$$

Note that for all the spatial domain HVS filters, we use a circular area of support.

Filter comparison

Here, we compare the luminance channel frequency domain filters, namely Nasenan's filter, Wandell's O_1 channel filter and Daly's HVS filter in 1D.

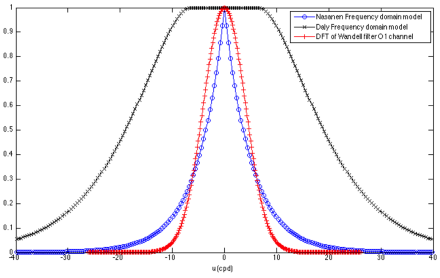

Figure 3. *Comparison between Wandell, Daly and Nasenan frequency domain filters*

Daly's frequency domain HVS model has a wide width compared to Nasenan's and wandell's. If we take the inverse fourier transform of Daly's luminance channel filter, the width of which is smaller compared with that of Nasanen's and Wandell's:

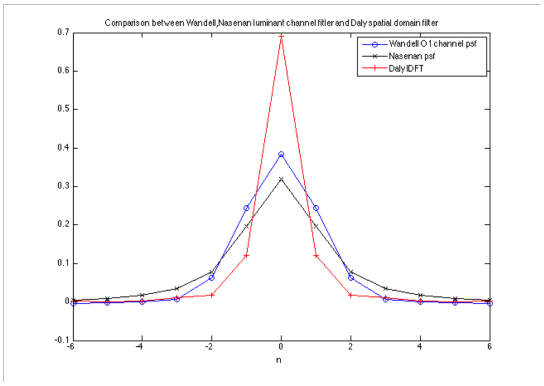

Figure 4. *Comparison between Wandell, Daly and Nasenan spatial domain filters*

First, we compare lumiance channel filters by examine the filtered result of a constant tone patch of size 512×512 that contains 50% cyan, 20% magenta, and 40% white, which is calculated in $Y_y C_x C_z$ color space, we setup the filter configurations as follows:

• Configuration 1: For luminance channel filter, we use Nasenan's model, for chrominance channel, we use the same filter for both red-green and blue-yellow channels as specified in (5).

• Configuration 2: Use Daly's model for luminance channel, chrominance channel filter is the same as Configuration 1.

• Configuration 3: Wandell's HVS filter models in $O_1 O_2 O_3$ color space.

• Configuration 4: Use Nasenan's model for luminance channel, for chrominance channel, we use separate filters for red-green (6) and blue-yellow channel (5).

Here, a scale factor $S = 3000$ is used. scale factor is defined as $S \equiv RD$, it is the product of resolution and viewing distance, the product of these two factors affect the halftone result.

First we compare the images halftoned using three different luminance channel filters: (a) Nasenan's luminance filter (Configuration 1), (b) Wandell's filter (Configuration 3), (c) Daly's luminance filter (Configuration 2).

Let the normalized error $E_{norm} = \sqrt{\frac{E}{height \times width}}$, where $height$ and $width$ are the height and width of the halftone image, and E is the error metric which is to be introduced in section III. E_{norm} of halftone using (a) filter is 1.4263. For (b), it has $E_{norm} = 5.2454$ and (c) has $E_{norm} = 1.9160$. So using Nasenan's luminance channel filter in $Y_y C_x C_z$ color space is better.

Next, we compare halftone results in $Y_y C_x C_z$ and $CIEL^* a^* b^*$ color spaces because these two color spaces are similar. The halftone in $Y_y C_x C_z$ color space is (a) and let halftone in $CIEL^* a^* b^*$ color space be (d). The halftone image of (a) has $E_{norm} = 1.4263$ and (d) has $E_{norm} = 1.4433$, they are very similar.

We also changed the gain factor of luminance channel filter on the overall error metric, we increased the gain factor g to four and compared with the original factor $g = 1$. Here, we still use Nasenan's lumiance channel filter (Configuration 1). The halftone image with gain factor 1 is (a) and let the halftone image with gain factor 4 be (e). The halftone image of (a) has $E_{norm} = 1.4263$ and (e) as $E_{norm} = 1.9696$. With $g = 1$, the halftone image is smoother and more homogeneous compared with that with $g = 4$.

We also compared the effect on halftone when we use single and separate filters for red-green and blue-yellow channels. The halftone of (a) is halftoned using single chrominance filter, and it has $E_{norm} = 1.4263$ and let the halftone using separate chrominance channel filters be (f), it has $E_{norm} = 1.3834$. We concluded that, using single chrominance channel filter for both red-green and blue-yellow channels is better in the sense that the pixels are arrange more homogeneously than using separate chrominance filters.

Color Direct Binary Search

Preliminaries

We use $[\mathbf{m}] = [m, n]^T$ to denote descrete coordinates and use $(\mathbf{x}) = (x, y)^T$ to denote continuous spatial coordi-

nates. In this paper, we use Neugebauer Primary (NP) to represent an image. First, we need to get the corresponding CIE XYZ values of the NPs using CIE XYZ color matching function (CMF), spectral reflectances of the NPs and we use D50 daylight illuminant. Let stimulus with respect to wavelength be $S(\lambda) = I(\lambda) \times R(\lambda)$, where $I(\lambda)$ is the illumiance, $R(\lambda)$ is the reflectance at wavelength λ. We get the CIE XYZ value by:

$$\begin{aligned} X &= \int S(\lambda)\bar{x}(\lambda)d\lambda \\ Y &= \int S(\lambda)\bar{y}(\lambda)d\lambda \\ Z &= \int S(\lambda)\bar{z}(\lambda)d\lambda \end{aligned} \tag{15}$$

Where $\bar{x}(\lambda)$,$\bar{y}(\lambda)$,$\bar{z}(\lambda)$ are the CMFs which represent the cone response functions (LMS).

We use 3-D vector valued function to represent a continuous tone image: $\mathbf{f}[\mathbf{m}] : \mathbb{R}^2 \rightarrow \mathbb{R}^3$. First, we get the $Y_yC_xC_z$ values corresponding to the CIE XYZ values by eq(3). Each sRGB value also corresponds to unique $Y_yC_xC_z$ values according to standard conversion. Thus we can obtain a Neugebauer Primary area coverage (NPAC) image set representation of a continuous-tone color image in $Y_yC_xC_z$ color space. According to Neugebauer's model of halftone color reproduction[9], the color of a halftone pattern represented by Neugebauer Primaries is:

$$T_c = \sum_{i=1}^{k^n} T_i a_i \tag{16}$$

Where $T \in Y_yC_xC_z$, is the color value in $Y_yC_xC_z$ color space, and $a_i \in [0,1]$, is area coverage of the ith Neugebauer Primary, $\sum a_i = 1$, c denotes the resulting halftone, n is the number of inks, and k is the number of levels per ink. For bilevel system with three types of inks, there are $2^3 = 8$ number of Neugebauer Primaries, which is used in this paper.

Initial Neugebauer Primary image

Given NPAC image set, which has as many planes as NPs, we can get initial Neugebauer Primary image (NP image) using random selection matrix, where each pixel is a ramdom number between 0 and 1.
Let $Ac[m,n,k]$ be the area coverage of the NPs in an NPAC image set, where k denotes NP, and $k \in [0, NP_{max}-1]$, where NP_{max} is the total number of NPs, and $[m,n]$ is the location of pixel on NPAC image, where $m \in [0, M-1]$ and $n \in [0, N-1]$, and M is the height, N is the width of the image. Let $r\ in [0,1]$ be a random number, and let p be the NP being selected for pixel $[m,n]$, where $p \in [0, NP_{max}-1]$, and p satisfy the following condition:

$$h[m,n] = \begin{cases} 0, & r \leq AC[m,n,0] \\ p, & lb < r \leq ub, p \geq 1. \end{cases} \tag{17}$$

where $lb = \sum_{k=0}^{p-1} Ac[m,n,k]$, and $ub = \sum_{k=0}^{p} Ac[m,n,k]$.

Note that the NPs are arranged in an order such that 0 represent the lightest, and $NP_{max}-1$ the darkest in visual weight. After repeating this process for all the pixels in an NPAC image, we get the initial NP halftone image.

Using existing selection matrix and NPAC image set to generate halftone is similar to how the initial Neigebauer Primary image is generated. Let $t[m,n]$ be the selection matrix, and $t[m,n] \in [0, L_{max}-1]$, where L_{max} is the maximum level in the selection matrix. The Neugebauer Primary being selected for pixel $[m,n]$, denoted p, satisfies:

$$h[m,n] = \begin{cases} 0, & \frac{l+1}{L_{max}+1} \leq AC[m,n,0] \\ p, & lb < \frac{l+1}{L_{max}+1} \leq ub, p \geq 1. \end{cases} \tag{18}$$

Where $l = t[m,n]$ and $l \in [0, L_{max}]$.

Color Direct Binary search Error metric

Similar to direct binary search (DBS), the color direct binary search (CDBS) also works by evaluating the error after each swap or toggle, but in order to preserve the average tone or color of the initial NP halftone image, we only allow swaps in CDBS. Our CDBS operates in opponent color space $Y_yC_xC_z$ as in A. Ufuk's work[2]. We evaluate the effect of swap on error metric in the neighborhood of 25 nearest pixels, if the trial swap reduce the error metric, we accept it. This process is repeated for each pixel until there's no more changes accepted.
Let $f_{Y_yC_xC_z}[\mathbf{m}]$ and $g_{Y_yC_xC_z}[\mathbf{m}]$ be the continuous-tone color image and halftone color imagein $Y_yC_xC_z$ color space,respectively. We represent each plane by $f_i[\mathbf{m}]$ and $g_i[\mathbf{m}]$, where $i = Y_y$,C_x,C_z. The error image between the original continuous-tone image and the halftone image is:

$$\begin{aligned} e_{Y_yC_xC_z}[\mathbf{m}] &\equiv f_{Y_yC_xC_z}[\mathbf{m}] - g_{Y_yC_xC_z}[\mathbf{m}] \\ e_i[\mathbf{m}] &\equiv f_i[\mathbf{m}] - g_i[\mathbf{m}], i = Y_y, C_x, C_z \end{aligned} \tag{19}$$

Assuming neighboring printer dot interaction is additive, and using the HVS filters in section II, the perceived error in $Y_yC_xC_z$ color space $\tilde{\mathbf{e}}_{Y_yC_xC_z}(\mathbf{x})$ with respect to continuous spatial coordinate $\mathbf{x}$ is:

$$\begin{aligned} &\tilde{\mathbf{e}}_{Y_yC_xC_z}(\mathbf{x}) = \sum_m diag(\tilde{p}_{spot\_Yy}(\mathbf{x} - \mathbf{Xm}), \\ &\tilde{p}_{spot\_Cx}(\mathbf{x} - \mathbf{Xm}), \tilde{p}_{spot\_Cz}(\mathbf{x} - \mathbf{Xm}))e_{Y_yC_xC_z}[\mathbf{m}] \end{aligned} \tag{20}$$

Where $\tilde{p}_{spot\_i}(\mathbf{x}) \equiv \tilde{p}_i(\mathbf{x}) * p_{spot}(\mathbf{x})$ is the ith component of the HVS filter point spread function convolved with the spot function of the printer, $\mathbf{X}$ is the periodicity matrix whose columns comprise the basis for the lattice of printer addressable dots. $diag(\cdot)$ is a diagonal matrix with elements listed between the parenthsis. But because the spot function of the printer has much smaller support than

HVS point spread function, we assume $\tilde{p}_{spot\_i}(\mathbf{x}) \approx \tilde{p}_i(\mathbf{x})$. Therefore, eq (20) can be approximated by:

$$\tilde{\mathbf{e}}_{Y_yC_xC_z}(\mathbf{x}) = \sum_m \tilde{\mathbf{P}}(\mathbf{x}-\mathbf{X}\mathbf{m}) e_{Y_yC_xC_z}[\mathbf{m}] \tag{21}$$

Where $\tilde{\mathbf{P}}(\mathbf{x}) \equiv diag(\tilde{p}_{YY}(\mathbf{x}), \tilde{p}_{Cx}(\mathbf{x}), \tilde{p}_{Cz}(\mathbf{x}))$. The error metric E is defined to be the total squared perceived errors of all three components of $Y_yC_xC_z$ color space.

$$E = \int \tilde{\mathbf{e}}_{Y_yC_xC_z}(\mathbf{x})^T \tilde{\mathbf{e}}_{Y_yC_xC_z}(\mathbf{x}) \tag{22}$$

Substitute (21) into eq (22):

$$E = \sum_m \sum_n \tilde{\mathbf{e}}_{Y_yC_xC_z}[\mathbf{m}]^T \left(\int \tilde{\mathbf{P}}(\mathbf{x}-\mathbf{X}\mathbf{m}) \tilde{\mathbf{P}}(\mathbf{x}-\mathbf{X}\mathbf{n}) \right) \times \tilde{\mathbf{e}}_{Y_yC_xC_z}[\mathbf{n}]. \tag{23}$$

The autocorrelation function of $\tilde{p}_i(\mathbf{x})$ is denoted $\mathbf{c}_{\tilde{p}\tilde{p}}(\mathbf{x})$, and the cross correlation function between $\tilde{p}_i(\mathbf{x})$ and $\tilde{e}_i(\mathbf{x})$ is denoted as $\mathbf{c}_{\tilde{p}\tilde{e}}(\mathbf{x})$. Then we can rewrite (23) as

$$\begin{aligned} E &= \sum_m \sum_n \tilde{\mathbf{e}}_{Y_yC_xC_z}[\mathbf{m}]^T \mathbf{c}_{\tilde{p}\tilde{p}}[\mathbf{m}-\mathbf{n}] \tilde{\mathbf{e}}_{Y_yC_xC_z}[\mathbf{n}]. \\ &= \sum_m \tilde{\mathbf{e}}_{Y_yC_xC_z}[\mathbf{m}]^T \mathbf{c}_{\tilde{p}\tilde{e}}[\mathbf{m}] \end{aligned} \tag{24}$$

Our goal is the minimize the perceived error E above, A. Ufuk and Allebach [2] performed DBS algorithm in $Y_yC_xC_z$ color space, they employed separate HVS models for luminance and chrominance channels, but they only used Nasenan's HVS model and a single HVS filter for both red-green and blue-yellow chanel. Here, we are going to compare several different models for each channel.

Next, we will talk about efficient evaluation of trial swaps on the error metric E (24).

Efficient evaluation of trial swap

Assuming that we have three-colorant cyan, magenta and yellow, there are 8 possible colorants for a bilevel printer. We order all the combinations from lightest to darkest in visual weight: W, Y, C, CY, M, MY, CM, CMY, where W stands for white when there are no prints on paper. We only perform swap because it preserves the average local color of the image. Let $\mathbf{m}_1$ and $\mathbf{m}_2$ be the trial swap halftone pixel locations, the changes at the swap locations in $Y_yC_xC_z$ color space at locations $\mathbf{m}_1$ and $\mathbf{m}_2$ are denoted by $\eth[\gtrdot_1]$ $\eth[\gtrdot_2]$. We define $\mathbf{A}[\mathbf{m}_1] \equiv diag(\mathbf{a}[\mathbf{m}_1])$ and $\mathbf{A}[\mathbf{m}_2] \equiv diag(\mathbf{a}[\mathbf{m}_2])$. Then the change in the error metric is:

$$\begin{aligned} \Delta E_s =& (\mathbf{a}[\mathbf{m}_1]^T \mathbf{A}[\mathbf{m}_1] + \mathbf{a}[\mathbf{m}_2]^T \mathbf{A}[\mathbf{m}_2]) \mathbf{c}_{\tilde{p}\tilde{p}}[0] \\ &+ 2\mathbf{a}[\mathbf{m}_1]^T \mathbf{c}_{\tilde{p}\tilde{e}}[\mathbf{m}_1] + 2\mathbf{a}[\mathbf{m}_2]^T \mathbf{c}_{\tilde{p}\tilde{e}}[\mathbf{m}_2] \\ &+ \mathbf{a}[\mathbf{m}_2]^T \mathbf{A}[\mathbf{m}_1] \mathbf{c}_{\tilde{p}\tilde{p}}[\mathbf{m}_2 - \mathbf{m}_1] \end{aligned} \tag{25}$$

Here we keep $\mathbf{c}_{\tilde{p}\tilde{p}}$ and $\mathbf{c}_{\tilde{p}\tilde{2}}$ as lookup tables, and if the trial swap is accepted, we update the $\mathbf{g}'_{Y_yC_xC_z}[\mathbf{m}]$ and $\mathbf{c}'_{\tilde{p}\tilde{e}}[\mathbf{m}]$ as:

$$\begin{aligned} \mathbf{g}'_{Y_yC_xC_z}[\mathbf{m}] =& \mathbf{g}_{Y_yC_xC_z}[\mathbf{m}] + \mathbf{a}[\mathbf{m}_1]\delta[\mathbf{m}-\mathbf{m}_1] \\ &+ \mathbf{a}[\mathbf{m}_2]\delta[\mathbf{m}-\mathbf{m}_2] \end{aligned} \tag{26}$$

$$\begin{aligned} \mathbf{c}'_{\tilde{p}\tilde{e}}[\mathbf{m}] =& \mathbf{c}_{\tilde{p}\tilde{e}}[\mathbf{m}] + \mathbf{A}[\mathbf{m}_1]\mathbf{c}_{\tilde{p}\tilde{p}}[\mathbf{m}-\mathbf{m}_1] \\ &+ \mathbf{A}[\mathbf{m}_2]\mathbf{c}_{\tilde{p}\tilde{p}}[\mathbf{m}-\mathbf{m}_2] \end{aligned} \tag{27}$$

Swapping neighborhood and time complexity reduction

Instead of swapping in a small neighborhood of 3×3. Here, the swap allowed is within 25×25 neighborhood, this allows more homogeneous halftone texture. Here's the monochrome halftone result if we allow swap only DBS in a neighborhood of 19×19:

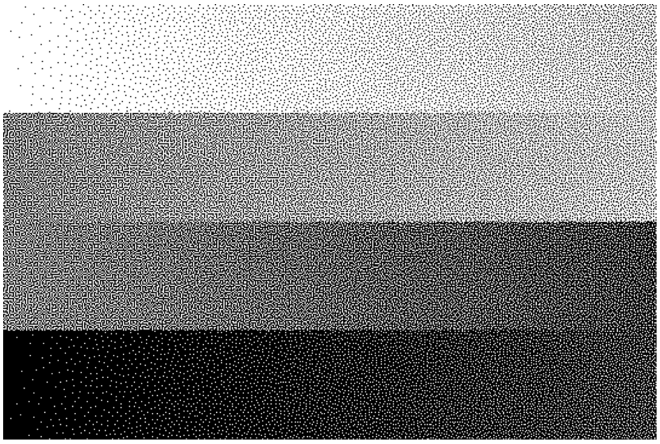

Figure 5. *monochrome DBS halftone with swap neighborhood of* 19×19.

Here's the halftone result when we increased the swapping neighborhood to 25×25:

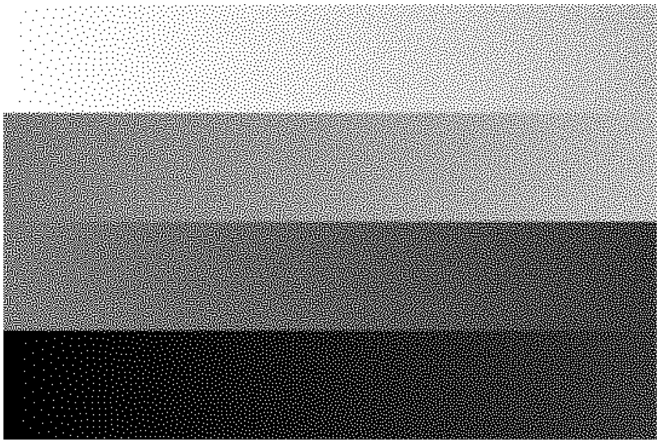

Figure 6. *monochrome DBS halftone with swap neighborhood of* 25×25.

It is clear that swapping in a neighborhood of 25×25 gives us more smooth halftone transitions. As Lieberman and Allebach [6] showed that the time complexity can be reduced by using $\mathbf{c}_{\tilde{p}\tilde{e}}$ LUT, by limiting the search of possible swaps to those in the anicausal neighborhood of a given pixel, and by partition pixels into small cells and process each cell a time in raster scan order.

Pipline of Getting NPAC Image from sRGB continuous Image

In order to enable NPAC-DBS to halftone images in sRGB color space, we need to represent sRGB values using Neugebauer Primaries, and there is a gamut mismatch between the two color spaces, which involves gamut mapping [7].

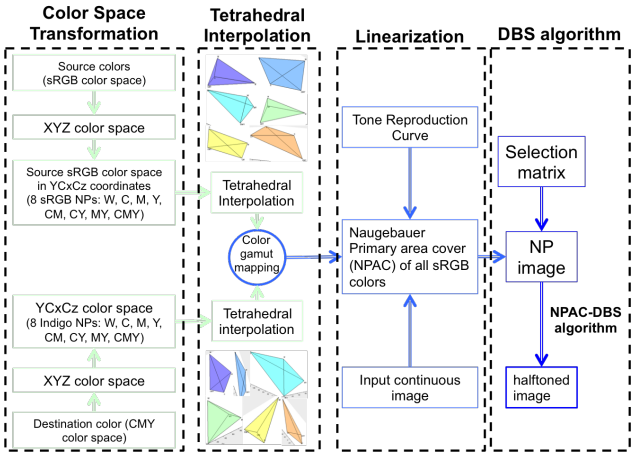

Figure 7. *The pipline of getting halftoned image*

Fig. 7 shows the flow chart of getting halftoned image from sRGB continuous image. As shown in this figure, we should getting NPAC image firstly as the data base of NPAC-DBS. This objective can be realized by 3 steps: 1). Color space transformation; 2). Tetrahedral interpolation and color gamut mapping; 3). linearization.

Color space transformation

To get printed halftone image from sRGB continuous image, we first define the sRGB color space as source color space, and Indigo press color space as destination color space. $Y_yC_xC_z$ color space is used because it is a linearized version of CIE $L^*a^*b^*$, and its linear structure is suitable for halftoning, because $Y_yC_xC_z$ color space preserves local averages. Therefore, the transformation from source and destination color space to $Y_yC_xC_z$ color space is performed, the formulas of which have been shown below (18-30).

In order to get coordinates in $Y_yC_xC_z$ color space, we should get the coordinates in XYZ color space first. We choose D50 as luminance, then the formula to transform from linear sRGB to XYZ is:

$$\begin{bmatrix} X \\ Y \\ Z \end{bmatrix} = [M] \begin{bmatrix} R \\ G \\ B \end{bmatrix} \tag{28}$$

Where

$$[M]^{-1} = \begin{bmatrix} 3.1338561 & -1.6168667 & -0.4906146 \\ -0.9787684 & 1.9161415 & 0.0334540 \\ 0.0719453 & -0.2289914 & 1.4052427 \end{bmatrix} \tag{29}$$

And the formula of transferring from XYZ to $Y_yC_xC_z$ color space is specified in (3), we rewrite it here as:

$$\begin{bmatrix} Y_y \\ C_x \\ C_z \end{bmatrix} = \begin{bmatrix} \frac{1}{X_w} & 0 & 0 \\ 0 & \frac{1}{Y_w} & 0 \\ 0 & 0 & \frac{1}{Z_w} \end{bmatrix} \begin{bmatrix} 0 & 116 & 0 \\ 500 & -500 & 0 \\ 0 & 200 & -200 \end{bmatrix} \begin{bmatrix} X \\ Y \\ Z \end{bmatrix} \tag{30}$$

Where X_w, Y_w, Z_w is the D_{50} white point.

In this paper, we only consider Cyan, Magenta, Yellow and their combinations of Indigo press as the destination primaries. So that, we have 8 NPs in total: white, yellow, cyan, cyan and yellow (green), magenta, magenta and yellow (red), cyan and magenta (blue) and cyan and magenta and yellow (black), we label the NPs as W,Y,C,CY,M,MY,CM,CMY.

Since, $Y_yC_xC_z$ is a linearized color space, the $Y_yC_xC_z$ coordinates of any sRGB colors are in the range or on the surface of polyhedrons, which is composed of 8 NPs. All the colors in destination color space are the combination of 8 destination NPs, so that the $Y_yC_xC_z$ coordinates of destination colors should also in the range or on the surface of polyhedrons composed of 8 destination NPs in theory. However, from Fig. 8, we can see the mismatch in destination $Y_yC_xC_z$ color space, which is caused by printer. We ignore this at present.

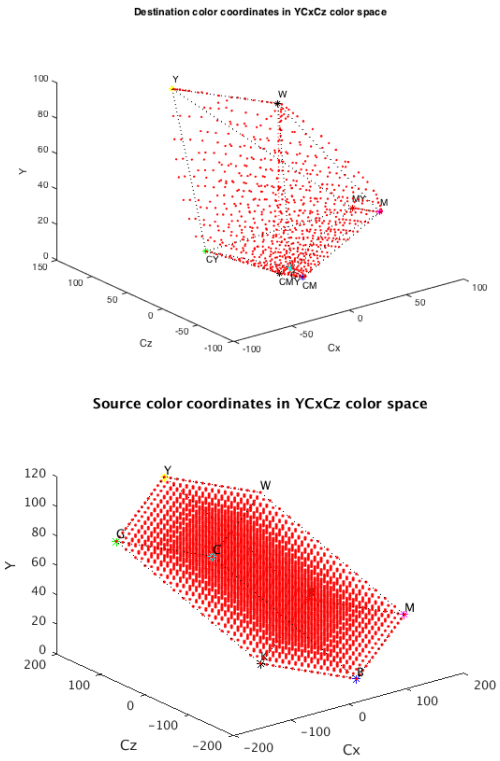

Figure 8. *Color gamut of source and destination $Y_yC_xC_z$ color space*

Tetrahedral interpolation and color gamut transformation

Both the source and destination $Y_yC_xC_z$ color gamut can be divided into several tetrahedrons in various ways. Choosing one dividing method: dividing the polyhedrons that are composed of 8 NPs into 6 tetrahedrons, the vertices of 6 tetrahedrons: W,C,M,CMY; W,C,Y,CMY; W,Y,MY,CMY; W,M,MY,CMY; C,M,CM,CMY; C,Y,CY,CMY. All the tetrahedrons corresponding to source and destination color space is shown is Fig. 9.

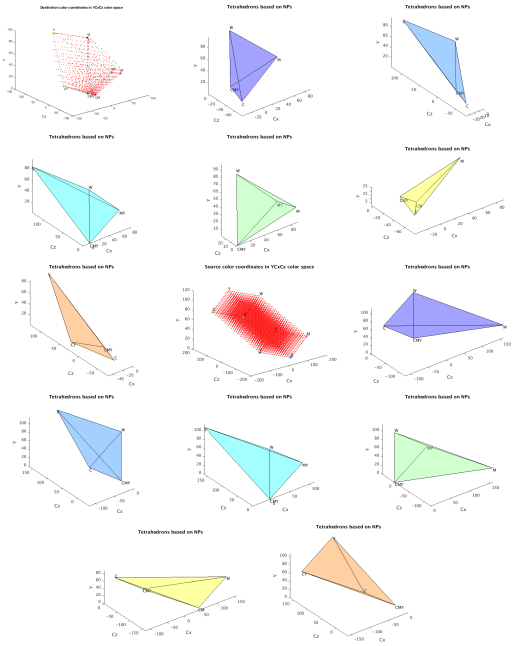

Figure 9. *Tetrahedral interpolation*

There are many color gamut mapping methods, but most of the methods need lots of calculation. As for the specificity of destination color space, which all the colors are decided by the 8 NPs, at the same time, and all the source colors also can be express by 8 NPs, so that the easiest and reasonable method to do the gamut mapping is just mapping the coordinates of 8 NPs between source and destination color space. In this condition, the tetrahedron that combined by same NPs between source and destination color space should be match one by one. The mapping relationship between tetrahedrons are shown in Fig. 10.

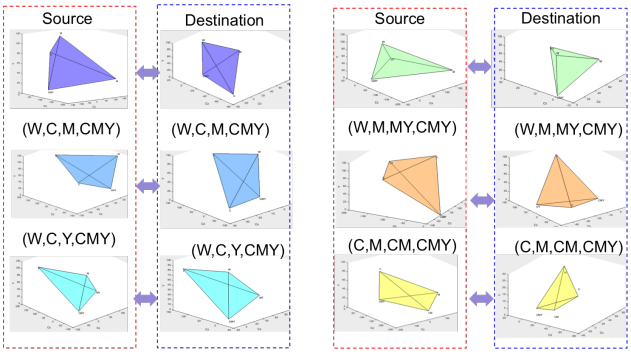

Figure 10. *Mapping between tetrahedrons of source and destination color space*

With the tetrahedron (W,C,M,CMY), for example, choosing the CMY as the origin point, and $W-CMY$, $C-CMY$, $M-CMY$ as the three space vectors, denote the three vector as $\vec{ox}$, $\vec{oy}$, $\vec{oz}$, so that all the points in the tetrahedron can be express by the combination of three vectors. Assuming, the coordinate of one color, which lies in tetrahedron (W,C,M,CMY), in source color space

is $p(Y_y, C_x, C_z)$, and the corresponding coordinate in destination color space is $p'(Y'_y, C'_x, C'_z)$. As for any color in source color space, we can get its coordinates in $Y_y C_x C_z$ color space easily based on the transformation from sRGB to XYZ, then to $Y_y C_x C_z$.

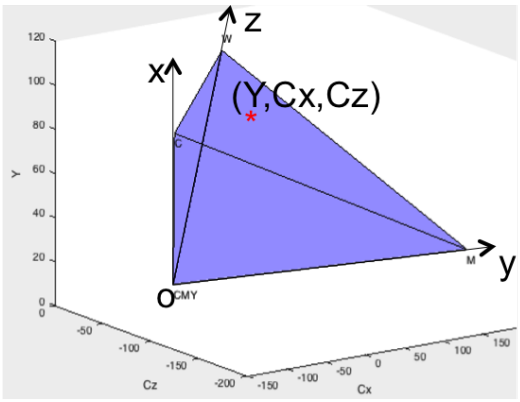

Figure 11. *Build the space coordinates system for tetrahedron*

Since, p is a point in or on the tetrahedron (W, C, M, CMY), the coordinate of p can be expressed by $\vec{ox}$, $\vec{oy}$, $\vec{oz}$.

Let, $(Y_y, C_x, C_z) = \alpha\vec{ox} + \beta\vec{oy} + \gamma\vec{oz}$, and $\delta = 1 - \alpha - \beta - \gamma$, where α, β, γ, δ are the percentages of C, M, W and CMY in source color space, then for any point in or on the tetrahedron, we must have the constraint conditions:

$$\begin{cases} 0 \le \alpha \le 1 \\ 0 \le \beta \le 1 \\ 0 \le \gamma \le 1 \\ 0 \le \delta \le 1 \end{cases} \tag{31}$$

Since, we mapping the coordinates of 8 NPs between source and destination color space, so that the coordinate of p' can be expressed as:

$$(Y'_y, C'_x, C'_z) = \alpha\vec{o'x'} + \beta\vec{o'y'} + \gamma\vec{o'z'} \tag{32}$$

$$\delta = 1 - \alpha - \beta - \gamma \tag{33}$$

Then, α, β, γ, δ are the percentages of C, M, W and CMY in destination color space.

In this method, any sRGB colors can be interpolated in one tetrahedron and be expressed by four NPs, and we can get the percentage of each of the four NPs easily.

linearization

Tone-Reproduction Curve (TRC) for correcting dot gain of printing process is used in this project. Fig. 12 show the process of getting the Tone-Reproduction Curve.

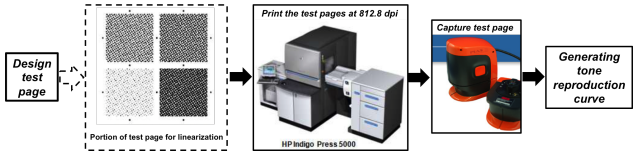

Figure 12. *Block diagram of the process for obtaining Tone-Reproduction Curve (TRC)*

In this paper, we choose 65 gray levels for generating the Tone-Reproduction Curve. To find the tone reproduction curve, we divide one test page into 4 subpages, and print 65 different gray level patterns for 4 times. The gray levels of the digital halftones are chosen as 0/255, 4/255, 8/255, ..., 248/255, 252/255, 255/255. We scan the printed halftone patterns using Personal Image Analysis System II (PIAS-II), and then calibrate the scanned image based on the nonlinear regression applied to PIAS-II: $Y_{x-rite} = a(\frac{RGB}{255})^b + c$, where RGB represents individually the R, G and B channel values returned by the PIAS-II. The coefficients of the power series for PIAS-II is shown in Table II, and the gray balance curves are shown in Fig. 13.

Coefficients of the power series for PIAS-II

PIAS-II			
coefficient	R	G	B
a	269.5	273.1	282.2
b	1.01	0.94	0.99
c	-11.25	-10.97	-8.20

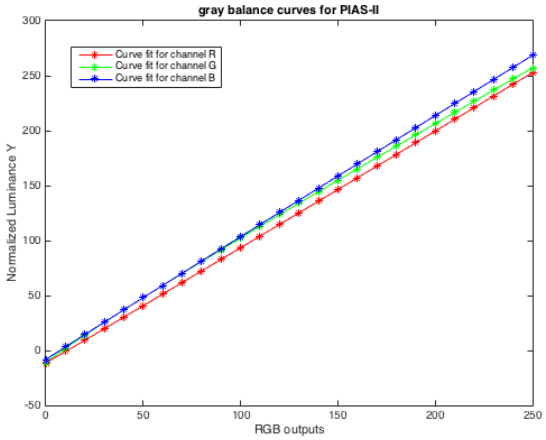

Figure 13. *Gray balance curves for PIAS-II using the coefficients in Table 2*

For each gray level, we average the printed absorptance values within the entire halftone pattern for this gray level. The tone reproduction curve which is the mapping of average gray value of the input halftone to averaged absorptance of the output print, is a piece-wise linear interpolation of 65 gray levels of digital halftones. The tone reproduction curve corresponding to Cyan is shown in Fig. 14.

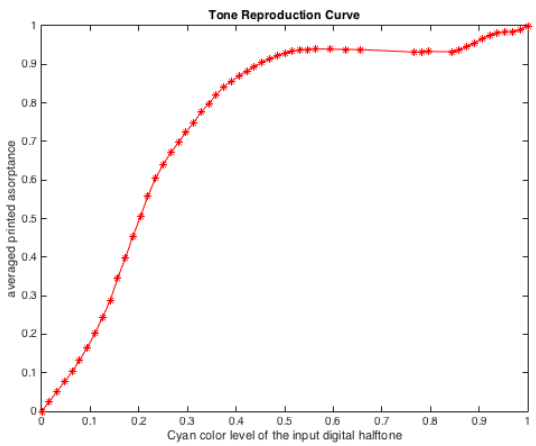

Figure 14. *Tone reproduction curve for Cyan*

Experimental results

Halftoning result of an image in sRGB color space

With Nasenan's luminance channel HVS filter and separate chrominance channel filters based on data collected by Mullen, we halftoned a colored image:

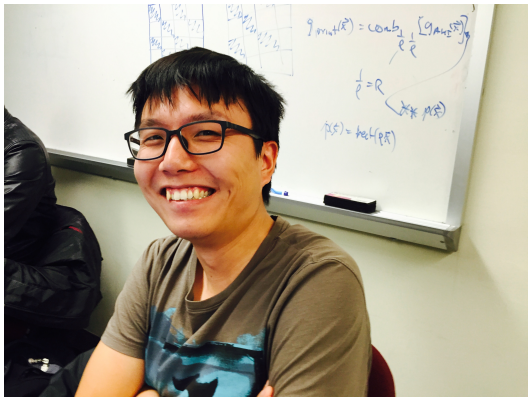

Figure 15. *Original image in sRGB color space.*

We have a selection matrix of size 256 × 256 which is generated by level-by-level monochrome DBS comprised of 255 levels, we can halftone the above image using the selection matrix, here's the halftone result:

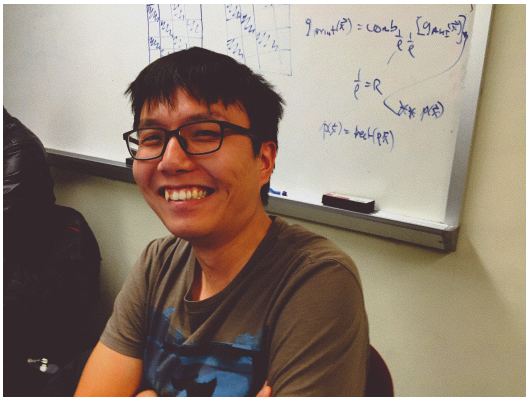

Figure 16. *Halftoned image using selection matrix.*

Halftoning the original image using NPAC-DBS results in a better halftone result:

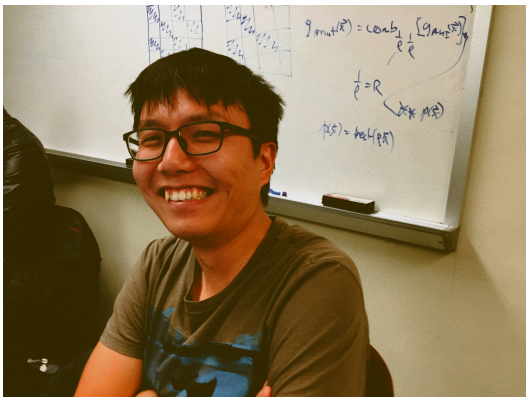

Figure 17. *Halftoned image using NPAC-DBS.*

Compared with halftoned image by selection matrix, NPAC-DBS is significantly better, especially in the glass area, it is more smooth and homogeneous than that of the selection matrix halftone. This is because NPAC-DBS has the knowledge of the image and halftone the image according to the texture, while selection matrix treat every pixel the same.

Halftoning colored bulls-eye image

Our halftoning method can minimize moire effect on halftoned image. The original color bulls-eye image is shown below.

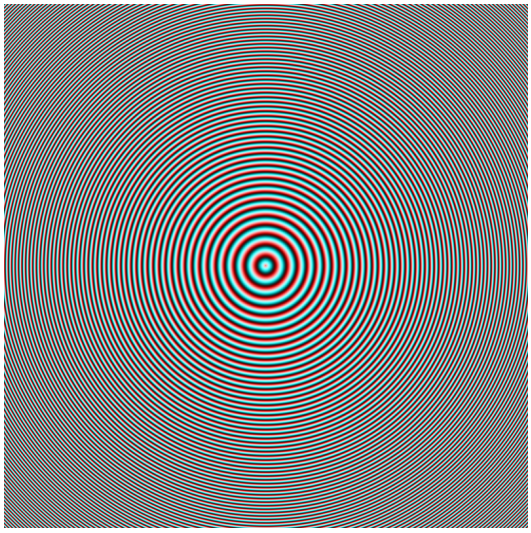

Figure 18. *Original bull eye image.*

Supercell method is a way to design screens $t[m,n]$, supercell enable us to deisgn accurately to form an angled screen, each cell in the screen is a cluster of pixels that form a cell. With dot profiles $p[m,n;b]$, where b is the graylevel of the dot profile, which generated using supercell method, we can generate a screen by:

$$t[m,n] = 255 - \sum_{b=0}^{255} p[m,n;b] \tag{34}$$

Using a periodical screen generated with supercell approach with parameters N1 = [9/2 -1;1 9/2] for yellow plane, N2 =[10/3 -10/3; 10/3 10/3] for Cyan plane and N3=[1 -9/2; 9/2 1] for Magenta plane to halftone the ripple image:

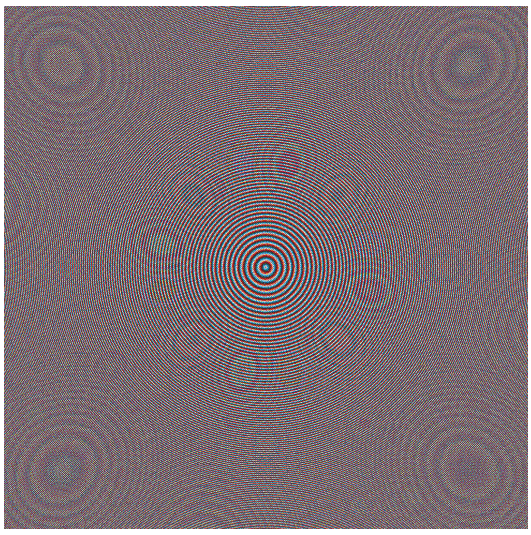

Figure 19. *Halftoned images using selection matrix wiht supercell approach*

The NPAC-DBS halftoned version of the moire image is shown below:

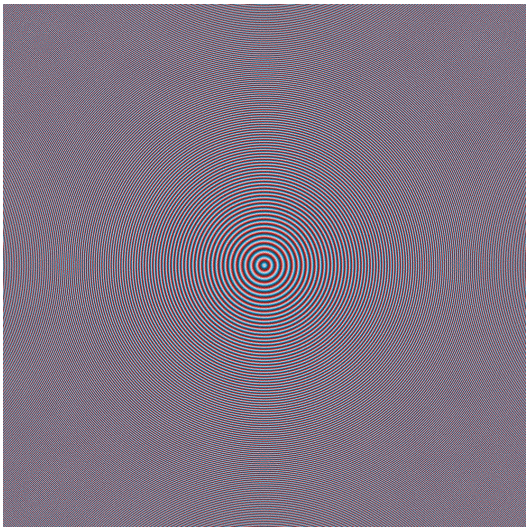

Figure 20. *NPAC-DBS halftoned image.*

Compared with screened halftone, the NPAC-DBS halftoned image do not have moire effect.

Discussion and Conclusions

We compared different HVS filter models and concluded that using Nasenan's model for luminance channel and using separate chrominance filters for red-green and blue-yellow channel yields a more homogeneous halftone image. We also concluded that setting the luminance channel amplification factor to be one is better than four. Instead of swapping in a neighborhood of 3×3, we swap in a 25 neighborhood, it also helped improving the quality of the halftoned image. Based on this observation, we developed NPAC-DBS algorithm that minimize the error metric in $Y_y C_x C_z$ color space. With sRGB to NPAC conversion pipeline, we are able to halftone any sRGB image using NPAC-DBS. We also observed that when there are closely arranged strip patterns in the original image, the moire is significantly reduced in the NPAC-DBS halftoned image. The set of Neugebauer Primaries can be potentially extended to support more colors than eight and render an image with wider gamut.

Acknowledgments

The authors wish to thank A. Jumabayeva for providing the periodic, clustered-dot screen sets used to generate Fig. 19.

References

[1] Je-Ho Lee and J. P. Allebach (2002, Oct.). CMYK Halftoning Algorithm Based on Direct Binary Search. *Journal of Electronic Imaging.* 11(4), pp. 517âĂŞ527.

[2] A. U. Agar and J. P. Allebach (2005, Dec.). Model-based color halftoning using direct binary search. *IEEE Transactions on Image Processing.* 14(12), pp. 1945-1959.

[3] T. Flohr, B. Kolpatzik, R. Balasubramanian, D. Carrara, C. Bouman, and J. Allebach. "Model-based color image quantization,". in *Proc. SPIE Human Vision, Visual Processing, and Digital Display IV*, vol. 1913 (1993), pp. 270-281.

[4] Zhang, Xuemei, and Brian A. Wandell (1997). A spatial extension of CIELAB for digital color image reproduction, *Journal of the Society for Information Display*. 5(1), pp: 61-63.

[5] Kim, Sang Ho, and Jan P. Allebach (2002). Impact of HVS models on model-based halftoning. *IEEE Transactions on Image Processing*. 11(3), pp.258-269.

[6] Lieberman, David J., and Jan P. Allebach (2000). A dual interpretation for direct binary search and its implications for tone reproduction and texture quality. *IEEE Transactions on Image Processing*. 9(11), pp:1950-1963.

[7] Morovič, J. "Title of chapter," in *Color Gamut Mappings*, *1*st ed. city: Wiley, 2008, pp. 978-0.

[8] Mullen, K. T. (1985). The Contrast Sensitivity of Human Colour Vision to Red-Green and Blue-Yellow Chromatic Gratings. *The Journal of Physiology*. 359(1), pp:381âĂŞ400.

[9] Morovič, Ján, Peter Morovič, and Jordi Arnabat. (2012). HANS: Controlling ink-jet print attributes via Neugebauer primary area coverages. *IEEE Transactions on Image Processing*. 21(2), pp:688-696.

[10] Peter Morovič, and Ján Morovič, and Jay Gondek, and Matthew Gaubatz, and Robert Ulichney. (2016). PARAWACS: color halftoning with a single selector matrix. *IS&TâĂŹs 24th Color and Imaging Conference (CIC24)*. Nov. 2016.

[11] Changhyung Lee. (2008). HYBRID SCREEN DESIGN AND AUTOMATIC PORTRAIT IMAGE ENHANCEMENT (Doctoral dissertation). Dec. 2008.

[12] Utpal Sarkar. (2015). HANS and PARAWACS. HP-Barcelona. 2015.

[13] Wandell, B.A. (2016). *Foundations of Vision.*.Sinauer Associates, 1995 [Online] Available: https://books.google.com/books?id=dVRRAAAAMAAJ

[14] Jan P. Allebach. (2001). DBS: retrospective and future directions. *Proc. SPIE, Color Imaging: Device-Independent Color, Color Hardcopy, and Graphic Arts VI*, Vol. 4300, pp. 358-376, 2001.

[15] Farhan A. Baqai and Jan P. Allebach. (2003). Halftoning via Direct Binary Search Using Analytical and Stochastic Printer Models. *IEEE Transactions on Image Processing*, Vol. 12(1), pp. 1057-7149, 2003.

[16] J. P. Allebach. (1999). *Selected Papers on Digital Halftoning.*, Bellingham, WA: SPIE Milestone Series, 1999.

[17] Ulichney. (1987). *Selected Papers on Digital Halftoning.*, Cambridge, MA, USA: MIT Press, 1987.

Author Biography

Wanling Jiang received her BS in Measurement and control technology and instrumentation from Dalian University of Technology (2011) and her MS degree in Electrical Engineering from University of Southern California (2013). Now, she is working on halftoning at Purdue University. Her work has focused on the optimization of halftone qualities.